

Strange magnetic form factor of the proton at $Q^2 = 0.23 \text{ GeV}^2$ *P. Wang^a, D. B. Leinweber^b, A. W. Thomas^{a,c}, and R. D. Young^d^a*Jefferson Laboratory, 12000 Jefferson Ave., Newport News, VA 23606 USA*^b*Special Research Center for the Subatomic Structure
of Matter (CSSM) and Department of Physics,
University of Adelaide 5005, Australia*^c*Department of Physics, College of William and Mary, Williamsburg VA 23187 USA and*^d*Physics Division, Argonne National Laboratory, Argonne, IL 60439, USA***Abstract**

We determine the u and d quark contributions to the proton magnetic form factor at finite momentum transfer by applying chiral corrections to quenched lattice data. Heavy baryon chiral perturbation theory is applied at next to leading order in the quenched, and full QCD cases for the valence sector using finite range regularization. Under the assumption of charge symmetry these values can be combined with the experimental values of the proton and neutron magnetic form factors to deduce a relatively accurate value for the strange magnetic form factor at $Q^2 = 0.23 \text{ GeV}^2$, namely $G_M^s = -0.034 \pm 0.021 \mu_N$.

PACS numbers: 13.40.-f; 14.20.-c 12.39.Fe; 11.10.Gh

arXiv:0807.0944v3 [hep-ph] 16 Jun 2009

* Notice: Authored by Jefferson Science Associates, LLC under U.S. DOE Contract No. DE-AC05-06OR23177. The U.S. Government retains a non-exclusive, paid-up, irrevocable, world-wide license to publish or reproduce this manuscript for U.S. Government purposes.

Strange quark contributions to the properties of the nucleon have attracted a lot of interest since the originally puzzling EMC results concerning the proton spin [1]. While that motivation has faded [2, 3], it remains a central issue in QCD, especially with respect to lattice QCD, where such terms necessarily involve so-called “disconnected graphs”, i.e., quark loops which are connected only by gluon lines to the valence quarks. Despite enormous effort [4], the *direct* lattice calculations of these contributions have so far been unable to produce a result which differs statistically from zero. On the other hand, by using the constraints of charge symmetry, which is expected to be accurate at the 1% level or better [5, 6], one can write relations (c.f. Eqs. (17) and (18), below) for the disconnected contributions to physical form factors [7] in terms of valence quantities, which *can* be accurately calculated in lattice QCD, and the experimentally determined form factors. In the case of the strange magnetic moment and charge radius of the proton, this approach has succeeded admirably [8, 9]. Here we apply the technique to the strange magnetic form factor at $Q^2 = 0.23 \text{ GeV}^2$.

Parity-violating electron scattering (PVES) has proven to be a valuable tool for experimentally determining the strange quark contribution to the electromagnetic form factors of the proton. Under the assumption of charge symmetry, one can deduce the strange electric or magnetic form factor ($G_{E,M}^s(Q^2)$) from measurements of the corresponding proton and neutron electromagnetic form factors *and* the neutral-weak vector form factor of the proton, through its contribution to PVES. While PVES measurements are very challenging, a number of groups have succeeded, starting with SAMPLE at Bates [10] and then A4 at Mainz [11] and G0 [12] and HAPPEX [13, 14, 15] at Jefferson Lab. A global analysis of all this data has given very precise values for the strange quark contribution to the proton magnetic moment, as well as its charge radius [16], which are consistent with the theoretical calculations mentioned above. The motivation for our current work is the knowledge that in the near future we expect new measurements from A4 and G0 at $Q^2 = 0.23 \text{ GeV}^2$.

In addition to the extensive experimental activity, a variety of theoretical models have been applied to the calculation of the strange nucleon form factors. These approaches include the QCD equalities supplemented with constituent quark model assumptions [17], heavy baryon chiral perturbation theory [18, 19], dispersive approaches [20, 21, 22], vector dominance model (VDM) [23], VDM with a kaon cloud contribution [24], the Skyrme model [25], the NJL model [26], the chiral soliton [27, 28], chiral bag [29] and chiral quark models [30, 31, 32], a two-component model with a meson cloud [33], etc. These theoretical predictions vary quite widely. For example, the predicted strange magnetic moment varies from relatively large and negative, -0.75 ± 0.30 [17] to sizeably positive, $+0.37$ [29].

As well as the above model calculations, there have been some lattice simulations of the strange magnetic moment, with early lattice simulations giving a relatively large negative value [7, 34, 35]. In 2003, Lewis *et al.* [4] used low order, quenched chiral perturbation theory, together with the lattice QCD simulation to calculate the strange form factors from lattice data. The magnetic form factor which they obtained at $Q^2 = 0.1 \text{ GeV}^2$ was $+0.05 \pm 0.06$. Recently, by combining the constraints of charge symmetry with new chiral extrapolation techniques and low mass, quenched lattice-QCD simulations of the individual quark contributions to the magnetic moments of the nucleon octet, a precise, non-zero value, $G_M^s(0) = -0.046 \pm 0.019$, was obtained [8].

In this paper, we present the lattice prediction for the strange magnetic form factor at $Q^2 = 0.23 \text{ GeV}^2$. We first extrapolate the u and d quark contributions to the proton magnetic form factor in quenched, heavy baryon chiral perturbation theory [36, 37]. The quenched lattice data from the CSSM Lattice Collaboration is used and finite range regularization

(FRR) is applied in the extrapolation, because of its improved convergence behavior at intermediate and large quark mass [38, 39, 40, 41, 42]. In the following we briefly introduce the chiral Lagrangian which is used in the extrapolation. The formal calculation of the magnetic form factor is then explained, followed by the numerical results.

There are many papers which deal with heavy baryon chiral perturbation theory. For details see, for example, Refs. [43, 44, 45]. For completeness, we briefly introduce the formalism here. In the heavy baryon chiral perturbation theory, the lowest order chiral Lagrangian for the baryon-meson interaction, which will be used in the calculation of the electromagnetic magnetic form factors, including the octet and decuplet baryons, is expressed as

$$\begin{aligned} \mathcal{L}_v = & i\text{Tr}\bar{B}_v(v \cdot \mathcal{D})B_v + 2D\text{Tr}\bar{B}_v S_v^\mu \{A_\mu, B_v\} + 2F\text{Tr}\bar{B}_v S_v^\mu [A_\mu, B_v] \\ & - i\bar{T}_v^\mu (v \cdot \mathcal{D})T_{v\mu} + \mathcal{C}(\bar{T}_v^\mu A_\mu B_v + \bar{B}_v A_\mu T_v^\mu), \end{aligned} \quad (1)$$

where S_μ is the covariant spin-operator, defined as

$$S_v^\mu = \frac{i}{2}\gamma^5\sigma^{\mu\nu}v_\nu. \quad (2)$$

Here, v^ν is the nucleon four velocity (in the rest frame, we have $v^\nu = (1, 0)$). D, F and \mathcal{C} are the coupling constants. The chiral covariant derivative, D_μ , is written as $D_\mu B_v = \partial_\mu B_v + [V_\mu, B_v]$. The pseudoscalar meson octet couples to the baryon field through the vector and axial vector combinations

$$V_\mu = \frac{1}{2}(\zeta\partial_\mu\zeta^\dagger + \zeta^\dagger\partial_\mu\zeta), \quad A_\mu = \frac{1}{2}(\zeta\partial_\mu\zeta^\dagger - \zeta^\dagger\partial_\mu\zeta), \quad (3)$$

where

$$\zeta = e^{i\phi/f}, \quad f = 93 \text{ MeV}. \quad (4)$$

The matrix of pseudoscalar fields, ϕ , is expressed as

$$\phi = \frac{1}{\sqrt{2}} \begin{pmatrix} \frac{1}{\sqrt{2}}\pi^0 + \frac{1}{\sqrt{6}}\eta & \pi^+ & K^+ \\ \pi^- & -\frac{1}{\sqrt{2}}\pi^0 + \frac{1}{\sqrt{6}}\eta & K^0 \\ K^- & \bar{K}^0 & -\frac{2}{\sqrt{6}}\eta \end{pmatrix}. \quad (5)$$

B_v and T_v^μ are the velocity dependent new fields, which are related to the original baryon octet and decuplet fields, B and T^μ , by

$$B_v(x) = e^{im_N \not{v} v_\mu x^\mu} B(x), \quad (6)$$

$$T_v^\mu(x) = e^{im_N \not{v} v_\mu x^\mu} T^\mu(x). \quad (7)$$

In the chiral $SU(3)$ limit, the octet baryons are degenerate. In our calculation we use the physical mass splittings for transition meson-baryon loop diagrams.

In the heavy baryon formalism, the propagators of the octet or decuplet baryon, j , are expressed as

$$\frac{i}{v \cdot k - \Delta + i\varepsilon} \quad \text{and} \quad \frac{iP^{\mu\nu}}{v \cdot k - \Delta + i\varepsilon}, \quad (8)$$

where $P^{\mu\nu}$ is $v^\mu v^\nu - g^{\mu\nu} - (4/3)S_v^\mu S_v^\nu$ and $\Delta = m_j - m_N$ is the mass difference between the baryon j and nucleon. The propagator of meson j ($j = \pi, K, \eta$) is the usual free propagator:

$$\frac{i}{k^2 - M_j^2 + i\varepsilon}. \quad (9)$$

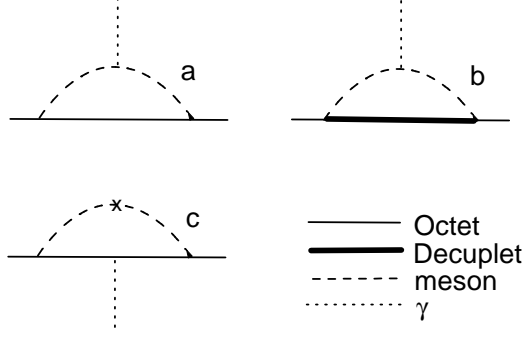


FIG. 1: Leading and next-to-leading order diagrams for the proton magnetic form factors. The last diagram, c, need only be included in the quenched case.

In the heavy baryon formalism, the electro-magnetic form factors are defined as:

$$\langle B(p') | J_\mu | B(p) \rangle = \bar{u}(p') \left\{ v_\mu G_E(Q^2) + \frac{i\epsilon_{\mu\nu\alpha\beta} v^\alpha S_v^\beta q^\nu}{m_N} G_M(Q^2) \right\} u(p), \quad (10)$$

where J_μ is the charge current, $q = p' - p$ and $Q^2 = -q^2$. In this paper, we focus on the magnetic form factors in each quark sector, aiming to extract the strange quark contribution.

With the Lagrangian given earlier, the leading and next-to-leading order diagrams for the magnetic form factor are shown in Fig. 1. In full QCD, the first diagram, a, is the leading diagram, while diagram b gives the next-to-leading order non-analytic term, because of the mass difference between octet and decuplet baryons. The last, or so-called double hair-pin, diagram need be considered only for the quenched case, where the η' is degenerate with the pion.

The contribution to the magnetic form factor of Fig. 1a is expressed as

$$G_M^a(Q^2) = \frac{-M_N \beta^a}{8\pi^3 f_\pi^2} \int d^3k \frac{k_y^2 u(\vec{k} + \vec{q}/2) u(\vec{k} - \vec{q}/2)}{\omega(\vec{k} + \vec{q}/2)^2 \omega(\vec{k} - \vec{q}/2)^2}. \quad (11)$$

$\omega_j(\vec{k}) = \sqrt{m_j^2 + \vec{k}^2}$ is the energy of the meson j . We regulate the loop integral using finite range regularisation, with $u(\vec{k})$ the ultra-violet regulator. Both the pion and koan are included in the calculation. In full QCD, the coefficients are obtained from the Lagrangian. In the quenched case the coefficients are obtained as in Refs. [36, 44, 46].

The contribution to the magnetic form factor of Fig. 1b can be written as

$$G_M^b(Q^2) = \frac{-M_N \beta^b}{8\pi^3 f_\pi^2} \int d^3k \frac{k_y^2 u(\vec{k} + \vec{q}/2) u(\vec{k} - \vec{q}/2) (\omega(\vec{k} + \vec{q}/2) + \omega(\vec{q}/2) + \omega(\vec{k} - \vec{q}/2))}{A}, \quad (12)$$

where

$$A = \omega(\vec{k} + \vec{q}/2) \omega(\vec{k} - \vec{q}/2) (\omega(\vec{k} + \vec{q}/2) + \Delta) (\omega(\vec{k} - \vec{q}/2) + \Delta) (\omega(\vec{k} + \vec{q}/2) + \omega(\vec{k} - \vec{q}/2)). \quad (13)$$

In the preceding equations, β^i ($i = a, b$) depends on the quark type, meson loop type and whether the calculation involves quenched or full QCD in the calculation.

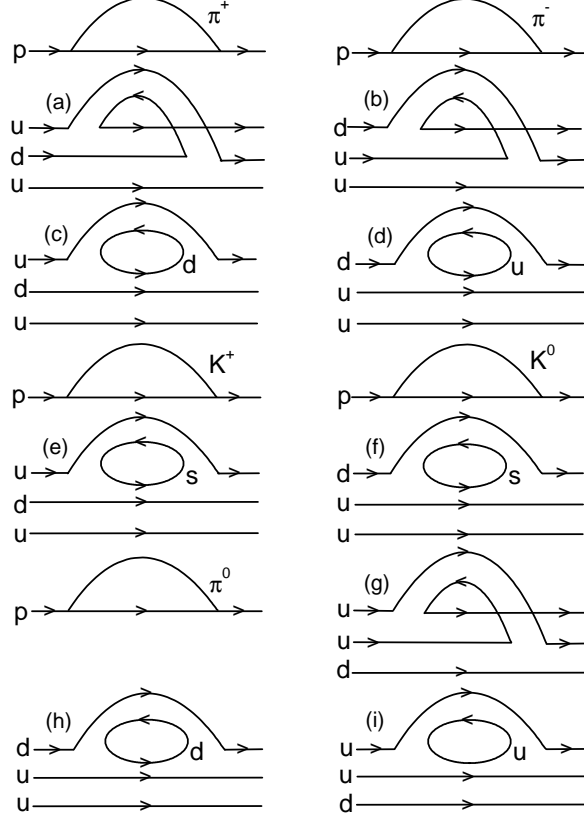


FIG. 2: Feynman diagrams at the quark level, which are included in Fig. 1a for the proton magnetic form factor.

In the quenched case, the additional double hair-pin term from the η' is expressed as

$$G_M^c(Q^2) = \frac{(3F - D)^2 M_0^2 G_M(Q^2)}{288\pi^3 f_\pi^2} \int d^3k \frac{\vec{k}^2 u(\vec{k})^2}{\omega(\vec{k})^5}, \quad (14)$$

where M_0 is the double hair-pin interaction strength. We note that the integral of Eq. (14) gives rise to a logarithmic divergence in the chiral limit. As a result we estimate the contribution of this graph using the renormalized value of $G_M(Q^2)$ obtained from the lattice simulation results at finite quark-mass values. Of course, in full QCD no such term need be included.

In the above formulas, the coefficients in quenched, valence and full QCD can be obtained with the same method as in Ref. [46]. For example, the diagram Fig. 1a is shown in detail in terms of the underlying quark lines in Fig. 2. In quenched QCD, the diagram with a quark loop has no contribution. In the case of valence quark sector, as well as the quenched diagram, the diagram with quark loop can also have contribution if the external photon field couples to the valence quark. In full QCD, both the valence and sea quark (loop) couple to the photon field. For the pion loop, in full QCD, Fig. 2a and Fig. 2c give contributions, while in the quenched case, Fig. 2a and Fig. 2b give contributions. The coefficients for Fig. 2c and Fig. 2i are the same as Fig. 2e, which is known from the Lagrangian, since QCD is flavor blind. For the same reason, the coefficients for Fig. 2d and Fig. 2h are the same as Fig. 2f.

TABLE I: Coefficients, β^a , for quarks in quenched, valence and full QCD for Fig. 1a. The left three columns are for an intermediate π meson and the right three columns are for an intermediate K meson.

quark	u	d	s	u	d	s
Quench	$-\frac{4}{3}D^2$	$\frac{4}{3}D^2$	0	0	0	0
Valence	$-4F^2 - \frac{8}{3}D^2$	$-\frac{2}{3}D^2 + 4DF - 2F^2$	0	$-\frac{1}{6}(3F + D)^2 \Lambda K$ $-\frac{1}{2}(D - F)^2 \Sigma K$	$-(D - F)^2$	0
Full QCD	$-(D + F)^2$	$(D + F)^2$	0	$-\frac{1}{6}(3F + D)^2 \Lambda K$ $-\frac{1}{2}(D - F)^2 \Sigma K$	$-(D - F)^2$	$\frac{1}{6}(3F + D)^2 \Lambda K$ $\frac{3}{2}(D - F)^2 \Sigma K$

TABLE II: Coefficients, β^b , for quarks in quenched, valence and full QCD for Fig. 1b. The left three columns are for an intermediate π meson and the right three columns are for an intermediate K meson.

quark	u	d	s	u	d	s
Quench	$-\frac{\mathcal{C}^2}{6}$	$\frac{\mathcal{C}^2}{6}$	0	0	0	0
Valence	$-\frac{\mathcal{C}^2}{18}$	$\frac{7\mathcal{C}^2}{18}$	0	$\frac{\mathcal{C}^2}{18}$	$\frac{\mathcal{C}^2}{9}$	0
Full QCD	$-\frac{2\mathcal{C}^2}{9}$	$\frac{2\mathcal{C}^2}{9}$	0	$\frac{\mathcal{C}^2}{18}$	$\frac{\mathcal{C}^2}{9}$	$-\frac{\mathcal{C}^2}{6}$

By subtracting the known coefficients from the total coefficients of full QCD, we can get the coefficient for each diagram in Fig. 2. The resulting coefficients for each quark for the different cases are summarized in Tables I and II.

As we know, most detailed lattice simulations for the nucleon electromagnetic form factors have been computed in the quenched approximation, in which the strange magnetic form factor is identically zero. Since the value in full QCD is not large, any direct calculation of G_M^s will require considerable effort to extract an accurate value. In this paper, we first concentrate on computing the contribution of each valence quark to the proton form factor, in the physical theory at the physical mass. Then by using charge symmetry and the experimental proton and neutron form factors, we are able to extract a precise value of strange magnetic form factor using the techniques of Refs. [7, 8].

The magnetic form factor can be expressed as

$$G_M(Q^2) = a_0 + a_2 m_\pi^2 + a_4 m_\pi^4 + \sum_{i=a}^c G_M^i(Q^2), \quad (15)$$

where the parameters a_0 , a_2 and a_4 can be obtained by fitting the quenched lattice data. In the numerical calculations, the SU(3) parameters are chosen to be $D = 0.76$ and $F = 0.50$ ($g_A = D + F = 1.26$) and the coupling constant \mathcal{C} is $-2D$. The FRR regulator, or form factor, $u(k)$, is taken to be a dipole ($u(k) = \frac{1}{(1+k^2/\Lambda^2)^2}$, with $\Lambda = 0.8$ GeV), although as shown by Young *et al.* [41] the model dependence associated with other choices is small.

We use SU(2) chiral symmetry, with only the light quark masses varying and the strange

quark mass fixed. Thus the K -meson mass is related to the pion mass by:

$$m_K^2 = \frac{1}{2}m_\pi^2 + m_K^2|_{\text{phy}} - \frac{1}{2}m_\pi^2|_{\text{phy}}, \quad (16)$$

which enables a direct relationship between the meson dressings of the magnetic form factor and the pion mass.

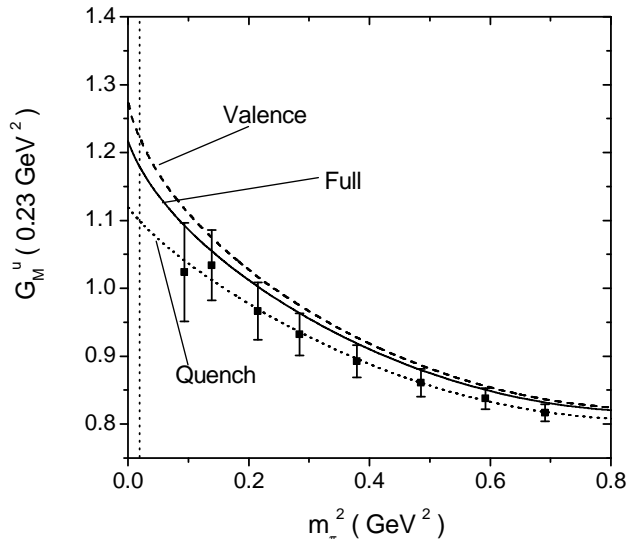


FIG. 3: The contribution of a single u quark, with unit charge, to the proton magnetic form factor at $Q^2 = 0.23 \text{ GeV}^2$ versus pion mass. The dotted, dashed and solid lines denote the quenched (finite volume), valence sector and full QCD (infinite volume) results, respectively.

The contribution of a single u quark with unit charge to the proton magnetic form factor is shown in Fig. 3. The dotted, dashed and solid lines are for the quenched, valence sector and full QCD results, respectively. The square points with error bars are the quenched lattice data obtained by the CSSM Lattice Collaboration [47]. The lattice results were fit with finite volume chiral perturbation theory followed by corrections to yield the infinite volume results. The FRR quenched chiral perturbation theory describes the lattice data results well over the range $m_\pi^2 \in 0.1 - 0.7 \text{ GeV}^2$. At the physical pion mass, the quenched (${}^qG_M^u$), valence (${}^vG_M^u$) and full QCD (${}^fG_M^u$) values of the magnetic form factor are 1.099 ± 0.165 , 1.221 ± 0.183 and 1.179 ± 0.177 , respectively.

In Fig. 4, we show the contribution of the d quark, with unit charge, to the proton magnetic form factor. The three styles of line have the same meaning as in Fig. 3. Again, the quenched lattice results are described very well. In contrast with the u quark case, the absolute value of the d quark contribution in full QCD is larger than that in the valence case. This is consistent with the disconnected contribution and hence the strange quark form factor being small and negative. At the physical pion mass, the quenched (${}^qG_M^d$), valence (${}^vG_M^d$) and full QCD (${}^fG_M^d$) values of the d quark contribution are -0.356 ± 0.053 , -0.383 ± 0.057 and -0.468 ± 0.070 , respectively.

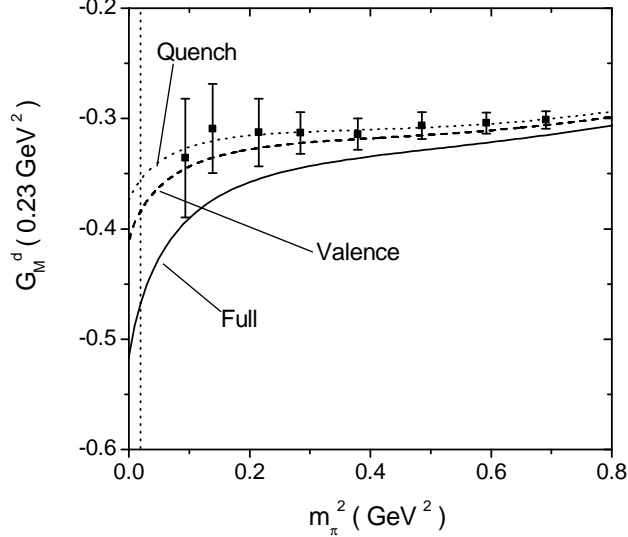


FIG. 4: The contribution of a d quark, with unit charge, to the proton magnetic form factor at $Q^2 = 0.23 \text{ GeV}^2$ versus pion mass. The dotted, dashed and solid lines denote the quenched (finite volume), valence sector and full QCD (infinite volume) results, respectively.

With the full QCD values of the u and d quark contributions, one can get the strange form factor by subtraction them from the proton or neutron magnetic form factor. However, because of the small value of G_M^s , the error bar obtained in this direct calculation is much larger than the central value of G_M^s . We therefore use the valence contributions, ${}^v G_M^u$ and ${}^v G_M^d$, which yield a relatively precise value of G_M^s .

The proton and neutron magnetic form factors can be written in terms of quark components as [7]

$$G_M^p = \frac{4}{3} {}^v G_M^u - \frac{1}{3} {}^v G_M^d + {}^l O_M^p, \quad (17)$$

$$G_M^n = \frac{2}{3} {}^v G_M^d - \frac{2}{3} {}^v G_M^u + {}^l O_M^n. \quad (18)$$

where ${}^l O_M^p = {}^l O_M^n = \frac{2}{3} {}^l G_M^u - \frac{1}{3} {}^l G_M^d - \frac{1}{3} G_M^s$. The label l denotes a “loop” or sea quark contribution, while the label v means a connected valence quark contribution in *full* QCD. In the equations above, charge symmetry has been used – i.e. the u and d quark contributions in the proton are the same as the corresponding d and u quark contributions in the neutron. Charge symmetry is known to be accurate at better than 1% where it has been tested, primarily in nuclear systems. It has to be assumed in order to extract the strange form factors from parity violating electron scattering. Under the assumption of charge symmetry, the strange quark contribution in the proton is the same as that in the neutron.

The contribution from the quark in the loop in Fig. 2 depends *only* on its mass – i.e. it is independent of whether the quark in the loop is labelled u , d or s . The loop contribution of each quark can be obtained using Eqs. (11) and (12) with the same coefficients $\frac{5}{3} D^2 - 2DF + 3F^2$ and $-\frac{C^2}{6}$. By calculation of the relevant loops using FRR, we evaluate the ratio ${}^l R_d^s = G_M^s / {}^l G_M^d$ at $Q^2 = 0.23 \text{ GeV}^2$. This yields the value ${}^l R_d^s = 0.185 \pm 0.038$ allowing the dipole mass parameter to vary between 0.6 and 1.0 GeV. Then, using Eqs. (17) and (18),

we find

$$G_M^s = \frac{{}^l R_d^s}{1 - {}^l R_d^s} (2G_M^p + G_M^n - 2{}^v G_M^u), \quad (19)$$

$$G_M^s = \frac{{}^l R_d^s}{1 - {}^l R_d^s} (G_M^p + 2G_M^n - {}^v G_M^d). \quad (20)$$

In Ref. [8], since we were working at $Q^2 = 0$, it was possible to use the measured magnetic moments of the nucleon and the hyperons. Since the hyperon magnetic form factors are not known at finite Q^2 , here we must use the extrapolated valence quark contributions (rather than ratios) to extract the strange form factor. The experimental values of $G_M^p(0.23)$ and $G_M^n(0.23)$ are $\frac{G_M^p(0.23)}{\mu_p G_D(0.23)} = 0.98 \pm 0.01$ [48] and $\frac{G_M^n(0.23)}{\mu_n G_D(0.23)} = 0.96 \pm 0.01$ [49], where G_D is the dipole function expressed as $G_D(Q^2) = 1/(1 + Q^2/0.71\text{GeV}^2)^2$. Substituting the experimental magnetic moment of the proton (2.793) and neutron (-1.913), we obtain the values $G_M^p(0.23) + 2G_M^n(0.23) = -0.534 \pm 0.036$ and $2G_M^p(0.23) + G_M^n(0.23) = 2.075 \pm 0.041$. Comparing the latter with twice the value of ${}^v G_M^u = 1.221 \pm 0.183$, obtained from our chiral analysis of the lattice results, it is clear that there is a significant cancellation in Eq. (19). Furthermore, the large value of $2{}^v G_M^u$ means that the corresponding error on $G_M^s(0.23)$ extracted from Eq. (19) will be large. Indeed, we find that Eq. (19) yields $G_M^s(0.23) = -0.083 \pm 0.092$. (Note that the quoted error bar arises from the errors in the lattice data, the experimental magnetic form factors and finally the theoretical uncertainty associated with FRR, especially the variation of the mass parameter Λ .) On the other hand, the relatively small value of ${}^v G_M^d = -0.383 \pm 0.057$ means that we obtain a much more accurate value of $G_M^s(0.23)$ using Eq. (20), namely $G_M^s(0.23) = -0.034 \pm 0.021$. We note that the two extracted values of G_M^s are consistent within their respective error bars and that the sign of both, negative, is consistent with the difference between the extrapolations of the single quark magnetic moments in the valence and full QCD cases in Figs. 3 and 4.

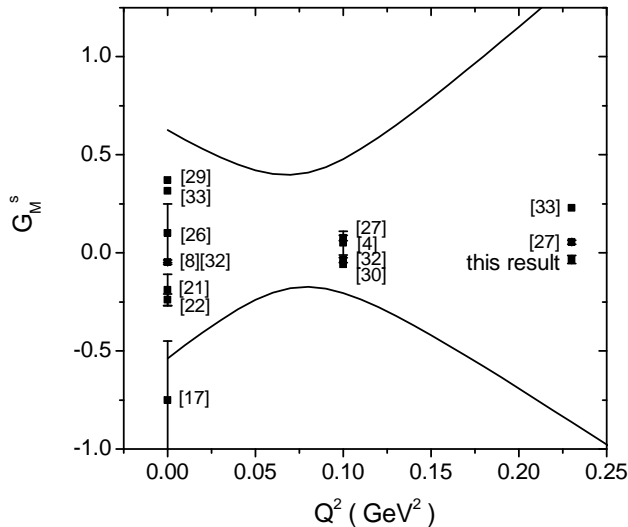


FIG. 5: Theoretical predictions of the strange magnetic form factors. The two lines are for the up and low limits of the experimental data with Eq. (21).

Some theoretical predictions for the strange magnetic form factor are shown in Fig. 5. These models give different values of G_M^s which are all within the current experimental error bars. As for the experimental values of G_M^s , using the same techniques as Ref. [16], we find:

$$G_M^s(Q^2) = 0.044 + 0.93Q^2 \pm \sqrt{0.34 - 7.02Q^2 + 47.8Q^4}, \quad (21)$$

where Q^2 is in GeV^2 . This form, which is the result of a global analysis of all published data [50], is valid over the range $0 < Q^2 < 0.3 \text{ GeV}^2$.

The issue of the errors in the strange magnetic moment were, of course, a serious issue in the earlier paper [8], and there and in the companion papers [51, 52] we explained all of the sources of error, including possible charge symmetry violation. The latter led to a much smaller contribution to the final error on G_M^s than the statistical errors on the lattice QCD data. This is also the case here at small but finite Q^2 . The dominance piece of the error which we quote to $G_M^s(0.23)$ arises from the errors on the lattice determination of ${}^v G_M^d$ and the experimental errors on proton and neutron magnetic form factors, in comparison with which the errors expected from all that is known about charge symmetry breaking in nuclear physics, namely that it is typically below 1%, really are negligible¹.

To conclude, we have extrapolated the lattice results for the separate valence quark contributions to the proton magnetic form factor at $Q^2 = 0.23 \text{ GeV}^2$ in quenched and full heavy baryon chiral perturbation theory. The leading and next-to-leading order diagrams are considered and all octet and decuplet baryons are included in the intermediate states. Finite-range regularisation is used in the one loop calculation, both because it improves the convergence of the chiral expansion and because it has been shown to permit a connection between quenched and dynamical lattice results [37]. By using the constraints of charge symmetry, we combine the extrapolated d valence quark contribution with the experimental proton and neutron magnetic form factors to obtain a surprisingly accurate determination of the strange magnetic form factor $G_M^s(0.23) = -0.034 \pm 0.021$. This is the first time it has proven possible to extract an accurate value of the strange magnetic form factor at $Q^2 = 0.23 \text{ GeV}^2$ using lattice QCD results. It will clearly be of considerable interest to compare this with the values which will be extracted from the recent A4 and G0 measurements at Mainz and JLab².

¹ We note that the size of the potential charge symmetry violation estimated in the calculation of Kubis and Lewis [53] is an exception, being an order of magnitude larger than that found in the earlier calculation by Miller [5, 54]. These authors used a very large anomalous omega-N coupling, in contrast with what we know from NN scattering. In addition, the omega coupling that they use (g_ω) is much larger than the usual one-boson exchange omega-N coupling. We also note that the implications of this work for other examples of charge symmetry violation have not yet been worked out. Nevertheless, if we were to use their extreme estimate, our result for $G_M^s(0.23)$ would change from -0.034 ± 0.021 to -0.025 ± 0.024 . The difference is very small and in view of the concerns already noted we prefer not to include this estimate of the charge symmetry correction in our final result.

² The latest measurement of strange quark contribution to the vector form factors was reported after this paper was submitted for publication [55]. The new result favors a negative strange magnetic form factor: $G_M^s(0.22\text{GeV}^2) = -0.14 \pm 0.11 \pm 0.11$.

Acknowledgements

We thank the Australian Partnership for Advanced Computing (APAC) and eResearch South Australia for supercomputer support enabling this project. This work is supported by the Australian Research Council and by U.S. DOE Contract No. DE-AC05-06OR23177, under which Jefferson Science Associates, LLC operates Jefferson Laboratory, and DE-AC02-06CH11357, under which UChicago Argonne, LLC operates Argonne National Laboratory.

-
- [1] J. Ashman *et al.* [European Muon Collaboration], Phys. Lett. B **206**, 364 (1988).
 - [2] F. Myhrer and A. W. Thomas, arXiv:0709.4067 [hep-ph].
 - [3] A. W. Thomas, Prog. Part. Nucl. Phys. **61**, 219 (2008) [arXiv:0805.4437 [hep-ph]].
 - [4] R. Lewis, W. Wilcox and R. M. Woloshyn, Phys. Rev. D **67**, 013003 (2003) [arXiv:hep-ph/0210064].
 - [5] G. A. Miller, Phys. Rev. C **57**, 1492 (1998) [arXiv:nucl-th/9711036].
 - [6] G. A. Miller, B. M. K. Nefkens and I. Slaus, Phys. Rept. **194**, 1 (1990).
 - [7] D. B. Leinweber and A. W. Thomas, Phys. Rev. D **62**, 074505 (2000) [arXiv:hep-lat/9912052].
 - [8] D. B. Leinweber *et al.*, Phys. Rev. Lett. **94**, 212001 (2005) [arXiv:hep-lat/0406002].
 - [9] D. B. Leinweber *et al.*, Phys. Rev. Lett. **97**, 022001 (2006) [arXiv:hep-lat/0601025].
 - [10] D. T. Spayde *et al.* [SAMPLE Collaboration], Phys. Lett. B **583**, 79 (2004) [arXiv:nucl-ex/0312016].
 - [11] F. E. Maas *et al.*, Phys. Rev. Lett. **94**, 152001 (2005) [arXiv:nucl-ex/0412030].
 - [12] D. S. Armstrong *et al.* [G0 Collaboration], Phys. Rev. Lett. **95**, 092001 (2005) [arXiv:nucl-ex/0506021].
 - [13] A. Acha *et al.* [HAPPEX collaboration], Phys. Rev. Lett. **98**, 032301 (2007) [arXiv:nucl-ex/0609002].
 - [14] K. A. Aniol *et al.* [HAPPEX Collaboration], Phys. Lett. B **635**, 275 (2006) [arXiv:nucl-ex/0506011].
 - [15] K. A. Aniol *et al.* [HAPPEX Collaboration], Phys. Rev. C **69**, 065501 (2004) [arXiv:nucl-ex/0402004].
 - [16] R. D. Young, J. Roche, R. D. Carlini and A. W. Thomas, Phys. Rev. Lett. **97**, 102002 (2006) [arXiv:nucl-ex/0604010].
 - [17] D. B. Leinweber, Phys. Rev. D **53**, 5115 (1996) [arXiv:hep-ph/9512319].
 - [18] T. R. Hemmert, U. G. Meissner and S. Steininger, Phys. Lett. B **437**, 184 (1998) [arXiv:hep-ph/9806226].
 - [19] T. R. Hemmert, B. Kubis and U. G. Meissner, Phys. Rev. C **60**, 045501 (1999) [arXiv:nucl-th/9904076].
 - [20] R. L. Jaffe, Phys. Lett. B **229**, 275 (1989).
 - [21] H. Forkel, Phys. Rev. C **56**, 510 (1997) [arXiv:hep-ph/9607452].
 - [22] H. W. Hammer, U. G. Meissner and D. Drechsel, Phys. Lett. B **367**, 323 (1996) [arXiv:hep-ph/9509393].
 - [23] S. Dubnicka, A. Z. Dubnickova and P. Weisenpacher, arXiv:hep-ph/0102171.
 - [24] T. D. Cohen, H. Forkel and M. Nielsen, Phys. Lett. B **316**, 1 (1993) [arXiv:hep-ph/9308374].
 - [25] N. W. Park, J. Schechter and H. Weigel, Phys. Rev. D **43**, 869 (1991).
 - [26] H. Weigel, A. Abada, R. Alkofer and H. Reinhardt, Phys. Lett. B **353**, 20 (1995)

- [arXiv:hep-ph/9503241].
- [27] A. Silva, H. C. Kim and K. Goeke, Phys. Rev. D **65**, 014016 (2002) [Erratum-ibid. D **66**, 039902 (2002)] [arXiv:hep-ph/0107185].
- [28] K. Goeke, H. C. Kim, A. Silva and D. Urbano, Eur. Phys. J. A **32**, 393 (2007) [arXiv:hep-ph/0608262].
- [29] S. T. Hong, B. Y. Park and D. P. Min, Phys. Lett. B **414**, 229 (1997) [arXiv:nucl-th/9706008].
- [30] L. Hannelius, D. O. Riska and L. Y. Glozman, Nucl. Phys. A **665**, 353 (2000) [arXiv:hep-ph/9908393].
- [31] L. Hannelius and D. O. Riska, Phys. Rev. C **62**, 045204 (2000) [arXiv:hep-ph/0001325].
- [32] V. E. Lyubovitskij, P. Wang, T. Gutsche and A. Faessler, Phys. Rev. C **66**, 055204 (2002) [arXiv:hep-ph/0207225].
- [33] R. Bijker, Rev. Mex. Fis. **S52N4**, 1 (2006) [arXiv:nucl-th/0701022].
- [34] S. J. Dong, K. F. Liu and A. G. Williams, Phys. Rev. D **58**, 074504 (1998) [arXiv:hep-ph/9712483].
- [35] N. Mathur and S. J. Dong, Nucl. Phys. Proc. Suppl. **94**, 311 (2001) [arXiv:hep-lat/0011015].
- [36] S. R. Sharpe, Phys. Rev. D **46**, 3146 (1992) [arXiv:hep-lat/9205020].
- [37] R. D. Young, D. B. Leinweber, A. W. Thomas and S. V. Wright, Phys. Rev. D **66**, 094507 (2002) [arXiv:hep-lat/0205017].
- [38] D. B. Leinweber, A. W. Thomas and R. D. Young, Phys. Rev. Lett. **92**, 242002 (2004) [arXiv:hep-lat/0302020].
- [39] W. Armour, C. R. Allton, D. B. Leinweber, A. W. Thomas and R. D. Young, J. Phys. G **32**, 971 (2006) [arXiv:hep-lat/0510078].
- [40] C. R. Allton, W. Armour, D. B. Leinweber, A. W. Thomas and R. D. Young, Phys. Lett. B **628**, 125 (2005) [arXiv:hep-lat/0504022].
- [41] R. D. Young, D. B. Leinweber and A. W. Thomas, Prog. Part. Nucl. Phys. **50**, 399 (2003) [arXiv:hep-lat/0212031].
- [42] P. Wang, D. B. Leinweber, A. W. Thomas and R. D. Young, Phys. Rev. D **75**, 073012 (2007) [arXiv:hep-ph/0701082].
- [43] E. E. Jenkins, M. E. Luke, A. V. Manohar and M. J. Savage, Phys. Lett. B **302**, 482 (1993) [Erratum-ibid. B **388**, 866 (1996)] [arXiv:hep-ph/9212226].
- [44] J. N. Labrenz and S. R. Sharpe, Phys. Rev. D **54**, 4595 (1996) [arXiv:hep-lat/9605034].
- [45] L. Durand, P. Ha and G. Jaczko, Phys. Rev. D **64**, 014008 (2001) [arXiv:hep-ph/0101267].
- [46] D. B. Leinweber, Phys. Rev. D **69**, 014005 (2004) [arXiv:hep-lat/0211017].
- [47] S. Boinepalli, D. B. Leinweber, A. G. Williams, J. M. Zanotti and J. B. Zhang, Phys. Rev. D **74**, 093005 (2006) [arXiv:hep-lat/0604022].
- [48] A. Bodek, S. Avvakumov, R. Bradford and H. Budd, Eur. Phys. J. C **53**, 349 (2008) [arXiv:0708.1946 [hep-ex]].
- [49] B. Anderson *et al.* [Jefferson Lab E95-001 Collaboration], Phys. Rev. C **75**, 034003 (2007) [arXiv:nucl-ex/0605006].
- [50] R. D. Young, R. D. Carlini, A. W. Thomas and J. Roche, Phys. Rev. Lett. **99**, 122003 (2007) [arXiv:0704.2618 [hep-ph]].
- [51] D. B. Leinweber, S. Boinepalli, A. W. Thomas, A. G. Williams, R. D. Young, J. B. Zhang and J. M. Zanotti, Eur. Phys. J. A **24S2** (2005) 79 [arXiv:hep-lat/0502004].
- [52] A. W. Thomas, R. D. Young and D. B. Leinweber, “Hadron structure on the back of an envelope,” in Proc. “1st Workshop on Quark-hadron Duality and the Transition to pQCD,” Frascati 2005, eds. A. Fantoni et al., 41-49 (2005) 9 pp. [arXiv:nucl-th/0509082]

- [53] B. Kubis and R. Lewis, Phys. Rev. C **74** (2006) 015204 [arXiv:nucl-th/0605006].
- [54] G. A. Miller, A. K. Opper and E. J. Stephenson, Ann. Rev. Nucl. Part. Sci. **56** (2006) 253 [arXiv:nucl-ex/0602021].
- [55] S. Baunack *et al.*, arXiv:0903.2733 [nucl-ex].